

# MERGERS AND NON-THERMAL PROCESSES IN CLUSTERS OF GALAXIES

**C. L. Sarazin**

University of Virginia

P.O. Box 3818, Charlottesville, VA 22903-0818, U.S.A.

SARAZIN@VIRGINIA.EDU

## Abstract

Clusters of galaxies generally form by the gravitational merger of smaller clusters and groups. Major cluster mergers are the most energetic events in the Universe since the Big Bang. The basic properties of cluster mergers and their effects will be discussed. Mergers drive shocks in the intracluster gas, and these shocks heat the intracluster gas, and should also accelerate nonthermal relativistic particles. Mergers also produce distinctive features in the X-ray images of clusters, including “cold fronts” and cool trails. Chandra and XMM/Newton observations of the X-ray signatures of mergers will be discussed. X-ray observations of shocks and cold fronts can be used to determine the geometry and kinematics of the merger. As a result of particle acceleration in shocks and turbulent acceleration following mergers, clusters of galaxies should contain very large populations of relativistic electrons and ions. Observations and models for the radio, extreme ultraviolet, hard X-ray, and gamma-ray emission from nonthermal particles accelerated in these shocks will also be described.

## 1 Introduction

Clusters of galaxies form hierarchically by the merger of smaller groups and clusters. Major cluster mergers are the most energetic events in the Universe since the Big Bang. In these mergers, the subclusters collide at velocities of  $\sim 2000$  km/s, releasing gravitational binding energies of as much as  $\gtrsim 10^{64}$  ergs. Figure 1 shows the Chandra image of the merging cluster Abell 85, which has two subclusters merging with the main cluster (Kempner, Sarazin, & Ricker 2002). The relative motions in mergers are moderately supersonic, and

shocks are driven into the intracluster medium. Figure 2 shows a numerical hydrodynamical simulation of the cluster merger, showing the hot shocks propagating through the merging clusters (Ricker & Sarazin 2001). In major mergers, these hydrodynamical shocks dissipate energies of  $\sim 3 \times 10^{63}$  ergs; such shocks are the major heating source for the X-ray emitting intracluster medium. Merger shocks heat and compress the X-ray emitting intracluster gas, and increase its entropy. We also expect that particle acceleration by these shocks will produce nonthermal electrons and ions, and these can produce synchrotron radio, inverse Compton (IC) EUV and hard X-ray, and gamma-ray emission.

## 2 Thermal effects of mergers

Mergers heat and compress the intracluster medium. Shocks associated with mergers also increase the entropy of the gas. Mergers can help to mix the intracluster gas, possibly removing abundance gradients. Mergers appear to disrupt the cooling cores found in many clusters; there is an anticorrelation between cooling core clusters and clusters with evidence for strong ongoing mergers (e.g., Buote & Tsai 1996). The specific mechanism by which cooling cores are disrupted is not completely understood at this time (e.g., Ricker & Sarazin 2001).

The heating and compression associated with mergers can produce a large, temporary increase in the X-ray luminosity (up to a factor of  $\sim 10$ ) and the X-ray temperature (up to a factor of  $\sim 3$ ) of the merging clusters (Figure 3; Ricker & Sarazin 2001; Randall, Sarazin, & Ricker 2002). Very luminous hot clusters are very rare objects in the Universe. Although major mergers are also rare events, merger boosts can cause mergers

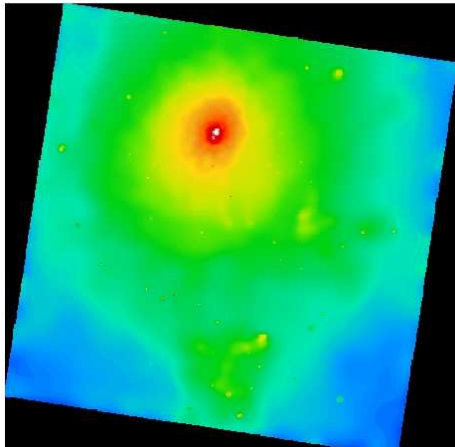


Figure 1: The Chandra X-ray image of the merging cluster Abell 85 (Kempner, Sarazin, & Ricker 2002). Two subclusters to the south and southwest are merging with the main cluster.

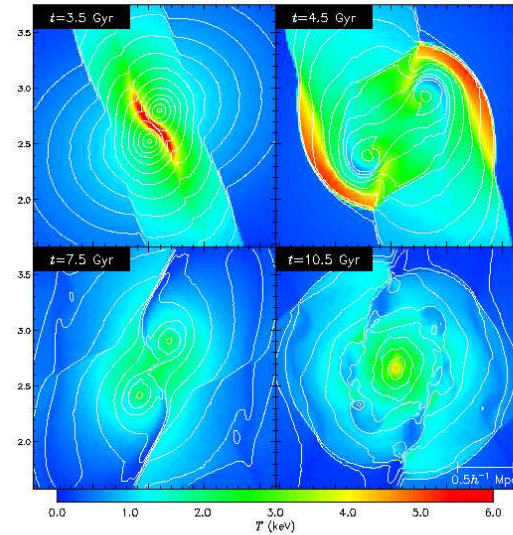


Figure 2: A hydrodynamical simulation of a cluster merger from Ricker & Sarazin (2001). The hot (red) regions are merger shocks.

to strongly affect the statistics of the most luminous, hottest clusters. Simulations predict that many of the most luminous, hottest clusters are actually merging systems, with lower total masses than would be inferred from their X-ray luminosities and temperatures (Randall et al. 2002). Since the most massive clusters give the greatest leverage in determining the cosmological parameters  $\Omega_M$  and  $\sigma_8$ , these values can be biased by merger boosts. Recent weak lensing studies appear to have confirmed these large merger boosts (e.g., Smith et al. 2003).

Cluster mergers can also boost the Sunyaev-Zeldovich effect and particularly the cross-section for a cluster to have strong lensing (Randall, Sarazin, & Ricker 2004; Torri et al. 2004).

### 3 Cold fronts and cool trails

One of the most dramatic results on clusters of galaxies to come from the Chandra X-ray observatory was the discovery of sharp surface brightness discontinuities in the images of merging clusters (Figures 1 & 4).

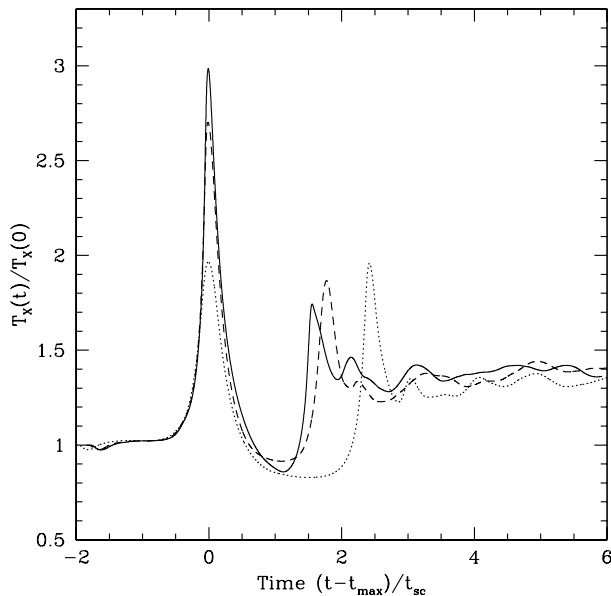


Figure 3: The X-ray emission-averaged temperature in a pair of equal mass clusters undergoing a merger (Ricker & Sarazin 2001; Randall et al. 2002). During a merger, the temperature can undergo a transient boost by up to a factor of three and the X-ray luminosity by up to a factor of ten.

These were first seen in Abell 2142 (Markevitch et al. 2000) and Abell 3667 (Vikhlinin, Markevitch, & Murray 2001b). Initially, one might have suspected these features were merger shocks, but X-ray spectral measurements showed that the dense, X-ray bright “post-shock” gas was cooler, had lower entropy, and was at the same pressure as the lower density “pre-shock” gas. This would be impossible for a shock. Instead, these “cold fronts” are apparently contact discontinuities between gas which was in the cool core of one of the merging subclusters and surrounding shocked intracluster gas (Vikhlinin et al. 2001b). The cool cores are plowing rapidly through the shocked cluster gas, and ram pressure sweeps back the gas at the front edge of the cold front. In a few cases (e.g., 1E0657-56; Figure 4; Markevitch et al. 2004), bow shocks are seen ahead of the cold fronts.

Cold fronts and merger shocks provide a number of classical hydrodynamical diagnostics which can be used to determine the kinematics of the merger (Vikhlinin et al. 2001b; Sarazin 2002). Most of these diagnostics give the merger Mach number  $\mathcal{M}$ . The standard Rankine-Hugoniot shock jump conditions can be applied to merger shocks; for example, the pressure

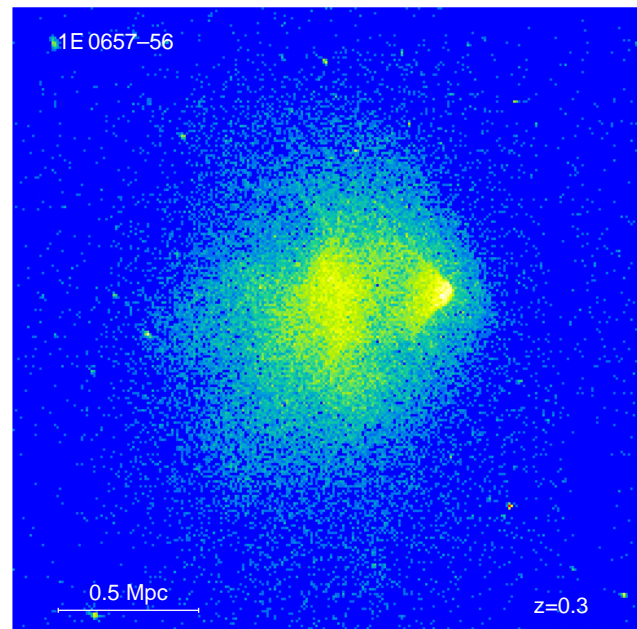


Figure 4: The Chandra X-ray image of the “bullet” cluster 1E0657-56 (Markevitch et al. 2004). The cluster shows a prominent cold front with a merger bow shock ahead (to the right) of it. (Figure kindly provided by Maxim Markevitch.)

discontinuity is

$$\frac{P_2}{P_1} = \frac{2\gamma}{\gamma+1} \mathcal{M}^2 - \frac{\gamma-1}{\gamma+1}, \quad (1)$$

where  $P_1$  and  $P_2$  are the pre- and post-shock pressure, and  $\gamma = 5/3$  is the adiabatic index of the gas. For bow shocks in front of cold front, the shock may be conical at the Mach angle,  $\theta_m = \csc^{-1}(\mathcal{M})$ . The ratio of the pressure at the stagnation point in front of a cold front to the pressure well ahead of it is given by

$$\frac{P_{st}}{P_1} = \begin{cases} \left(1 + \frac{\gamma-1}{2} \mathcal{M}^2\right)^{\frac{\gamma}{\gamma-1}}, & \mathcal{M} \leq 1, \\ \mathcal{M}^2 \left(\frac{\gamma+1}{2}\right)^{\frac{\gamma+1}{\gamma-1}} \left(\gamma - \frac{\gamma-1}{2\mathcal{M}^2}\right)^{-\frac{1}{\gamma-1}}, & \mathcal{M} > 1. \end{cases} \quad (2)$$

If the motion of the cold front is supersonic, the stand-off distance between the cold front and the bow shock varies inversely with  $\mathcal{M}$ . For major mergers, these kinematic diagnostics generally indicate that mergers are mildly transonic  $\mathcal{M} \approx 2$ , corresponding to merger velocities of  $\sim 2000$  km/s.

Mergers also provide a useful environment for testing the role of various physical processes in clusters. For example, the very steep temperature gradients at cold fronts imply that thermal conduction is suppressed by a large factor ( $\sim 10^2$ ; Ettori & Fabian 2000; Vikhlinin,

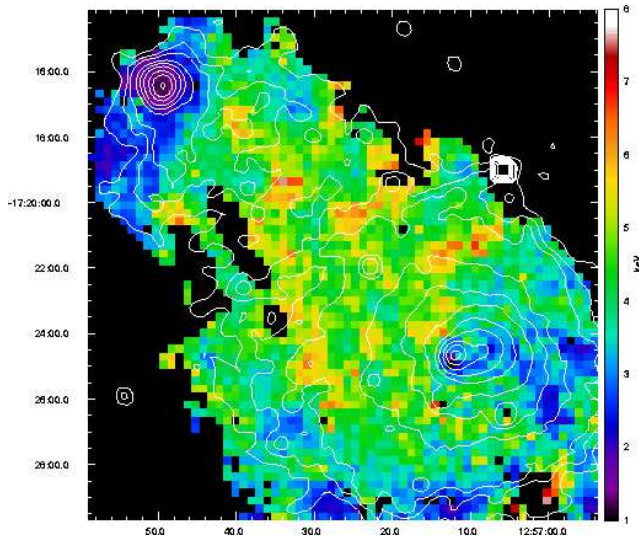


Figure 5: An X-ray temperature map (colors) of the merging cluster Abell 1644 from the XMM/Newton observation of Reiprich et al. (2004). The contours show the X-ray surface brightness. A trail of cooling gas lies below the subcluster at the northeast corner of the image.

Markevitch, & Murray 2001a), presumably by magnetic fields. The smooth front surfaces of some cold fronts suggest that Kelvin-Helmholtz instabilities are being suppressed, also probably by magnetic fields. Recently, Markevitch et al. (2004) have used the relative distributions of dark matter, galaxies, and gas in the dramatic merging cluster 1E0657-56 (Figure 4) to argue that the collision cross-section per unit mass of the dark matter must be low,  $\sigma/m \lesssim 1 \text{ cm}^2/\text{g}$ , which excludes most of the self-interacting dark matter models invoked to explain the mass profiles of galaxies.

In addition to merger cold fronts, cool trails of X-ray gas have been seen behind merging subclusters in some Chandra and XMM/Newton observations. For example, Figure 5 shows the XMM/Newton X-ray temperature map of the merging cluster Abell 1644 (Reiprich et al. 2004). A trail of cooler gas lies below (behind) the merging subcluster. Presumably, this gas was stripped from the subcluster during the merger. Figure 6 shows the results of a numerical hydrodynamical simulation of a cluster merger by Eric Tittley (Reiprich et al. 2004). The simulation shows a cool trail very similar to that in Abell 1644.

#### 4 Non-thermal effects of mergers

High speed astrophysical shocks in diffuse gas generally lead to significant acceleration of relativistic elec-

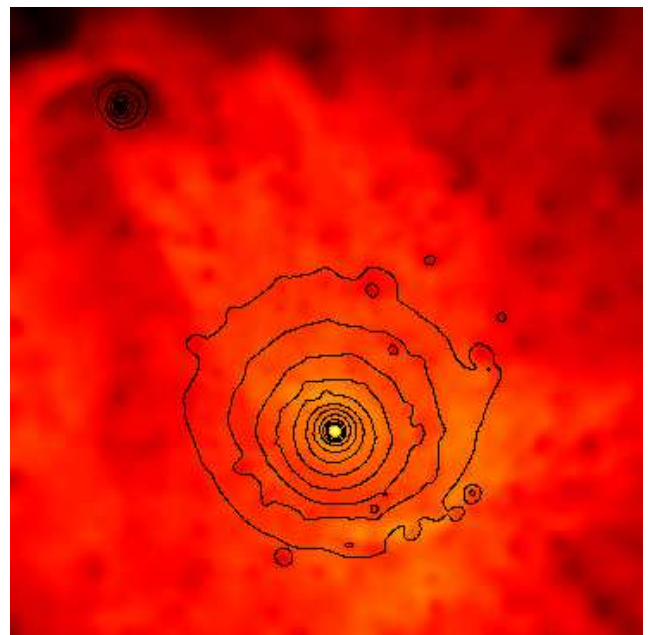


Figure 6: A temperature map (yellow hot, dark cold) from a hydrodynamical simulation of a merging cluster (Reiprich et al. 2004), showing a cool trail behind the merging cluster. The contours show the X-ray surface brightness. Although the simulation was constructed independently of the observation of Abell 1644 (Figure 5), the temperature map and X-ray image are similar.

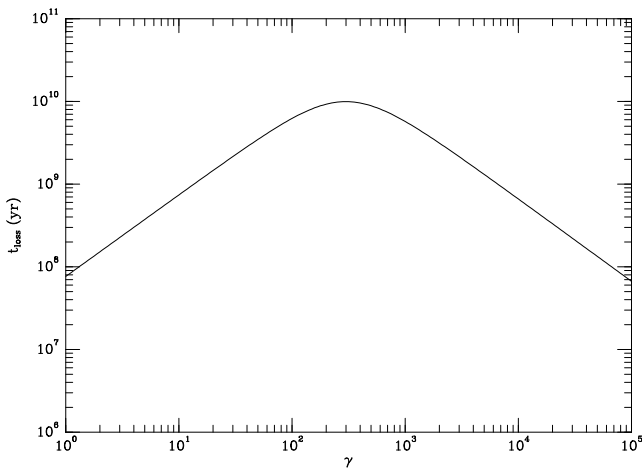


Figure 7: The lifetimes of relativistic electrons in a typical cluster as a function of their Lorentz factor  $\gamma$  (Sarazin 1999a). The lifetime is maximum for  $\gamma \sim 300$ .

trons. For example, typical supernova remnants have blast wave shock velocities of a few thousand km/s, which are comparable to the speeds in merger shocks. (However, the Mach numbers in merger shocks are much lower.) The ubiquity of radio emission from Galactic supernova remnants implies that at least a few percent of the shock energy goes into accelerating relativistic electrons, with more probably going into ions. If these numbers are applied to strong merger shocks in clusters, one would expect that relativistic electrons with a total energy of  $E_{\text{rel,e}} \sim 10^{62}$  erg would be accelerated, with even more energy in the relativistic ions. Thus, merging clusters should have huge populations of relativistic particles.

Clusters may contain both primary and secondary relativistic electrons. Primary electrons are accelerated directly in mergers. Secondary electrons are produced by the interactions of relativistic ions with thermal ions in the intracluster medium. Collisions between relativistic ions (mainly protons) and thermal ions (also mainly protons) can produce pions (and other mesons):

$$p + p \rightarrow p + p + n\pi. \quad (3)$$

The charged pions decay to produce electrons and positrons:

$$\begin{aligned} \pi^\pm &\rightarrow \mu^\pm + \nu_\mu(\bar{\nu}_\mu) \\ \mu^\pm &\rightarrow e^\pm + \bar{\nu}_\mu(\nu_\mu) + \nu_e(\bar{\nu}_e). \end{aligned} \quad (4)$$

In mergers, primary relativistic particles may be produced through shock acceleration or by turbulent ac-

celeration, where the turbulence may have been generated by a merger shock passage. Often, it is argued that cluster radio relics are due to shock acceleration, while cluster radio halos are produced by turbulent acceleration. Although the seed particles for acceleration could come from the thermal intracluster gas, it is easier to re-accelerate a relic population of low energy relativistic particles.

However they are produced, clusters should retain some of these relativistic particles for very long times. The cosmic rays gyrate around magnetic field lines, which are frozen-in to the gas, which is held in by the strong gravitational fields of clusters. Because clusters are large, the timescales for diffusion are generally longer than the Hubble time. The low gas and radiation densities in the intracluster medium imply that losses by relativistic ions are very slow, and those by relativistic electrons are fairly slow.

Figure 7 shows the loss timescale for electrons under typical cluster conditions; electrons with Lorentz factors  $\gamma \approx 300$  and energies of  $\approx 150$  MeV have lifetimes which approach the Hubble time, as long as cluster magnetic fields are not too large ( $B \lesssim 3 \mu\text{G}$ ). On the other hand, the higher energy particles which produce radio synchrotron emission and could produce hard X-ray emission have relatively short lifetimes, comparable to the durations of cluster mergers. As a result, clusters should contain two populations of primary relativistic electrons accelerated in mergers: those at  $\gamma \sim 300$  which have been produced by mergers over the lifetime of the clusters; and a tail to higher energies produced by any current merger.

Figure 8 shows the energy spectrum of primary electrons in an example of a model for a cluster undergoing a merger (Sarazin 1999a). There is a large population of low energy electrons ( $\gamma \sim 300$ ,  $E \sim 150$  MeV), which were accelerated in earlier mergers in the same cluster. There is also an approximately power-law tail of higher particles in the electron distribution; these electrons are being accelerated in the current merger.

The IC emission spectrum from the electrons in this model is shown in Figure 9. The lower energy electrons ( $\gamma \sim 300$ ) will mainly be visible in the EUV/soft X-ray range (e.g., Sarazin & Lieu 1998). Because these low energy electrons have very long lifetimes, they should be present in most clusters. Such EUV/soft X-ray emission has been apparently been seen in several clusters (e.g., Nevalainen et al. 2003; Bowyer et

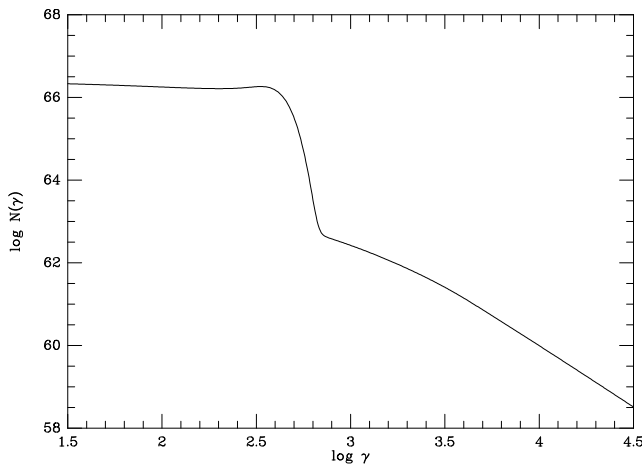


Figure 8: The energy spectrum of relativistic electrons in a model for a merging cluster (Sarazin 1999a). The large population at  $\gamma \sim 300$  are due to many previous mergers, while the tail to high energies is due to the current merger.

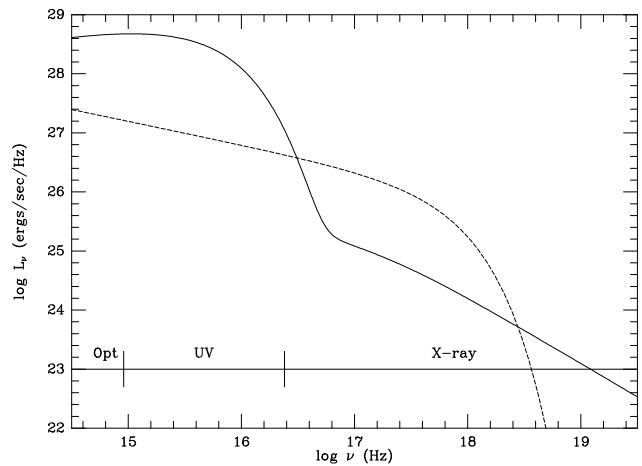


Figure 9: The IC spectrum produced by the electrons in the model for a merging cluster in Figure 8. For reference, the dashed line is thermal bremsstrahlung at a typical cluster luminosity.

al. 2004), although its origin is uncertain and may well be thermal (e.g., Kaastra et al. 2003).

More energetic electrons, with energies of many GeV, produce hard X-ray IC emission and radio synchrotron emission. Diffuse radio sources, not associated with radio galaxies, have been observed for many years in merging clusters (see the review by Feretti in this volume). Centrally located, unpolarized, regular sources are called “radio halos”, while peripheral, irregular, polarized sources are called “radio relics”. Radio halos and relics are only found in clusters which are undergoing mergers. Recent Chandra observations seem to show a direct connection between radio halos and merger shocks in clusters (Markevitch & Vikhlinin 2001; Govoni et al. 2004; see also the papers by Feretti and by Markevitch in this volume).

The radio power in cluster radio halos correlates very strongly with the X-ray luminosity and X-ray temperature of clusters (e.g., Bacchi et al 2003; Liang et al. 2000). The correlation is much stronger than expected based on a simple scaling of cluster properties (e.g., Kempner & Sarazin 2001). This strong correlation might be explained if the radio-emitting electrons are due to merger shock or turbulent acceleration, and if the high X-ray luminosities and temperatures are due to the transient boosts which occur during mergers (Randall et al. 2002; Randall & Sarazin 2004).

The same higher energy electrons responsible for the

radio emission will produce hard X-ray IC emission. Recently, such emission appears to have been detected with BeppoSAX and RXTE in at least Coma (Fusco-Femiano et al. 1999; Rephaeli, Gruber, & Blanco 1999), Abell 2256 (Fusco-Femiano et al. 2000; Rephaeli & Gruber 2003), and Abell 754 (Fusco-Femiano et al. 2003). However, the detections are relatively weak and controversial (Fusco-Femiano et al. 2004; Rossetti & Molendi 2004). Observations with INTEGRAL may help to resolve the nature of the hard excesses in clusters by providing higher spatial resolution hard X-ray images.

One of the difficulties in detecting nonthermal hard X-ray excesses in clusters of galaxies is the very strong thermal emission from clusters. As noted above, clusters with radio halos tend to be particularly hot (Liang et al. 2000), which only adds to this difficulty. One possible way around this difficulty would be to find cooler groups with radio halos; then, the contrast of the hard X-ray IC emission with the group thermal emission would be more favorable. A survey for radio halos in groups and follow-up hard X-ray observations might be useful. It is possible that one case may have been detected already in IC 1262 (Hudson & Henriksen 2003).

I believe one of the most exciting possibilities for the future is the detection of clusters in hard gamma-ray radiation (Figure 10). Essentially, all models for the non-thermal populations in clusters predict that they should

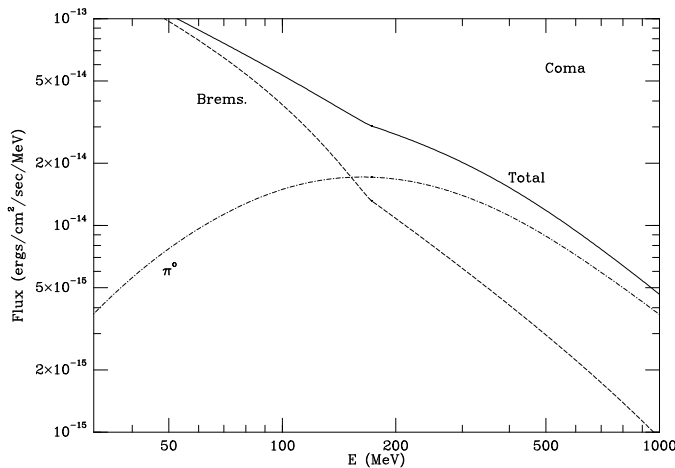
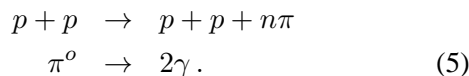


Figure 10: The gamma-ray emission spectrum from a model for relativistic particles in the Coma cluster (Sarazin 1999b). The emission from electrons (mainly bremsstrahlung in this model) and ions (due to  $\pi^0$  decays) are shown separately.

be very luminous gamma-ray sources, particularly at photon energies of  $\sim 100$  MeV (Sarazin 1999b; Gabici & Blasi 2004). The emission at these energies is partly due to electrons with energies of  $\sim 150$  MeV, which should be ubiquitous in clusters. One nice feature of this spectral region is that emission is produced both by relativistic electrons (through bremsstrahlung and IC emission) and relativistic ions. The ions (mainly protons) produce gamma-rays by  $\pi^0$  decay; the process is similar to the secondary electron production process in Eq. (3) & (4):



Both the emissivity of bremsstrahlung by relativistic electrons and that of gamma-ray emission by  $\pi^0$  decay involve collisions with the ions in the thermal intra-cluster gas; thus, the ratio of the two emission mechanisms depends mainly on the ratio of relativistic electrons to relativistic ions. Since the two emission mechanisms have different spectral shapes and are expected to be of comparable importance, one can determine separately both population in clusters. Models suggest that GLAST and AGILE will detect  $\gtrsim 40$  nearby clusters (e.g., Gabici & Blasi 2004).

## Acknowledgments

I would like to thank my collaborators, who have included Liz Blanton, Tracy Clarke, Josh Kempner, Scott Randall, Thomas Reiprich, Paul Ricker, and Eric Tittley. I thank Maxim Markevitch for providing Figure 4. This work was supported by the National Aeronautics and Space Administration through Chandra Award Numbers GO2-3159X, GO3-4155X, GO3-4160X, GO4-5149X, and GO4-5150X, and XMM/Newton Award Numbers NAG5-13737 and NAG5-13088.

## References

- Bacchi, M., Feretti, L., Giovannini, G., & Govoni, F. 2003, *A&A*, 400, 465
- Bowyer, S., Korpela, E. J., Lampton, M., Jones, T. W. 2004, *ApJ*, 605, 168
- Buote, D. A., & Tsai, J. C. 1996, *ApJ*, 458, 27
- Ettori, S., & Fabian, A. C. 2000, *MNRAS*, 317, L57
- Fusco-Femiano, R., et al., 1999, *ApJ*, 513, L21
- Fusco-Femiano, R., et al., 2000, *ApJ*, 534, L7
- Fusco-Femiano, R., et al., 2003, *A&A*, 398, 441
- Fusco-Femiano, R., Orlandini, M., Brunetti, G., Feretti, L., Giovannini, G., Grandi, P., & Setti, G. 2004, *ApJ*, 602, L73
- Gabici, S., & Blasi, P. 2004, *Aph*, 20, 579
- Govoni, F., Markevitch, M., Vikhlinin, A., VanSpeybroeck, L., Feretti, L., & Giovannini, G. 2004, *ApJ*, 605, 695
- Hudson, D. S., & Henriksen, M. J. 2003, *ApJ*, 595, L1
- Kaastra, J. S., Lieu, R., Tamura, T., Paerels, F. B. S., & den Herder, J. W. 2003, *A&A*, 397, 445
- Kempner, J., & Sarazin, C. L. 2001, *ApJ*, 548, 639
- Kempner, J., Sarazin, C. L., & Ricker, P. R. 2002, *ApJ*, 579, 236
- Liang, H., Hunstead, R. W., Birkinshaw, M., & Andreani, P. 2000, *ApJ*, 544, 686
- Markevitch, M., et al., 2000, *ApJ*, 541, 542
- Markevitch, M., et al., 2004, *ApJ*, in press (astro-ph/0309303)
- Markevitch, M., & Vikhlinin, A. 2001, *ApJ*, 563, 95
- Nevalainen, J., Lieu, R., Bonamente, M., & Lumb, D. 2003, *ApJ*, 584, 716
- Randall, S. W., & Sarazin, C. L. 2004, preprint
- Randall, S. W., Sarazin, C. L., & Ricker, P. M. 2002, *ApJ*, 577, 579
- Randall, S. W., Sarazin, C. L., & Ricker, P. M. 2004, preprint

- Reiprich, T. H., Sarazin, C. L., Kempner, J. C., & Tittley, E. 2004, ApJ, in press (astro-ph/0308282)
- Rephaeli, Y., & Gruber, D. 2003, ApJ, 579, 587
- Rephaeli, Y., Gruber, D., & Blanco, P. 1999, ApJ, 511, L21
- Ricker, P. M., & Sarazin, C. L. 2001, ApJ, 561, 621
- Rossetti, M., & Molendi, S. 2004, A&A, 414, L41
- Sarazin, C. L. 1999a, ApJ, 520, 529
- Sarazin, C. L. 1999b, in Diffuse Thermal and Relativistic Plasma in Galaxy Clusters, ed. H. Böhringer, L. Feretti, & P. Schuecker (Garching: MPE Rep. 271), 185
- Sarazin, C. L. 2002, in Merging Processes in Clusters of Galaxies, ed. L. Feretti, I. M. Gioia, & G. Giovannini (Dordrecht: Kluwer), 1
- Sarazin, C. L., & Lieu, R. 1998, ApJ, 494, L177
- Smith, G. P., Edge, A. C., Eke, V. R., Nichol, R. C., Smail, I., & Kneib, J.-P. 2003, ApJ, 590, L79
- Torri, E., Meneghetti, M., Bartelmann, M., Moscardini, L., Rasia, E., & Tormen, G. 2004, MNRAS, 349, 476
- Vikhlinin, A., Markevitch, M., & Murray, S. M. 2001a, ApJ, 549, L47
- Vikhlinin, A., Markevitch, M., & Murray, S. M. 2001b, ApJ, 551, 160